

Higgs results and prospects at ATLAS

S. ROSATI

INFN, Sezione di Roma - Roma, Italy

received 7 January 2015

Summary. — Highlights of a selection of the recent results of Run-1 measurements of the Higgs boson properties, with the ATLAS experiment at LHC, are presented. The results have been obtained with up to 25 fb^{-1} of proton-proton collisions at center of mass energy of 7 and 8 TeV. Prospects in the field of Higgs properties measurements, with the data that will be collected at the future LHC runs, with up to 3000 fb^{-1} , are also discussed.

PACS 14.80.Bn – Standard-model Higgs boson.

1. – Introduction

The observation of a new particle in the search for a Standard Model (SM) Higgs boson [1-3], reported by the ATLAS [4] and CMS [5] Collaborations, was a major milestone of the wide LHC Physics program.

In this document, the actual status of the measurements of the properties of the boson, with the ATLAS experiment, is presented, together with a review of the prospective for the measurements in the future LHC runs. The ATLAS detector is described in [6].

2. – Measurement of the Higgs boson mass

The two channels $H \rightarrow ZZ^{(*)} \rightarrow \ell^+\ell^-\ell^+\ell^-$ and $H \rightarrow \gamma\gamma$ allow the full reconstruction of the final state Higgs decay and the precision measurement of the resonance mass. The invariant mass distribution of the candidate events used for the mass fit in the two channels is shown in fig. 1. The measured mass is for each of the two channels:

$$m_H^{\gamma\gamma} = 126.8 \pm 0.2 \text{ (stat)} \pm 0.7 \text{ (syst)} \text{ GeV},$$
$$m_H^{4\ell} = 124.3_{-0.5}^{+0.6} \text{ (stat)}_{-0.3}^{+0.5} \text{ (sys)} \text{ GeV}.$$

The combination of the two masses is done allowing the signal strength to vary independently between the two channels, and fixing the ratios of the cross sections of

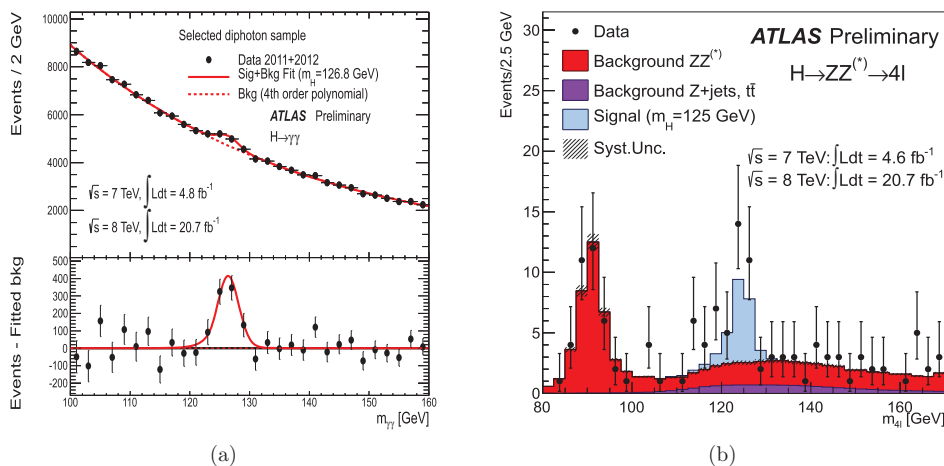


Fig. 1. – Invariant mass distributions for the $H \rightarrow \gamma\gamma$ and $H \rightarrow ZZ^{(*)} \rightarrow \ell^+\ell^-\ell^+\ell^-$ selected candidates for the combined 7 TeV and 8 TeV data. (a) Invariant mass distribution of the diphoton candidates. The result of a fit to the data with both signal and background components is superimposed. (b) The distribution of the four-lepton invariant mass compared to the background expectation and the signal expectation for a $m_H = 125$ GeV hypothesis.

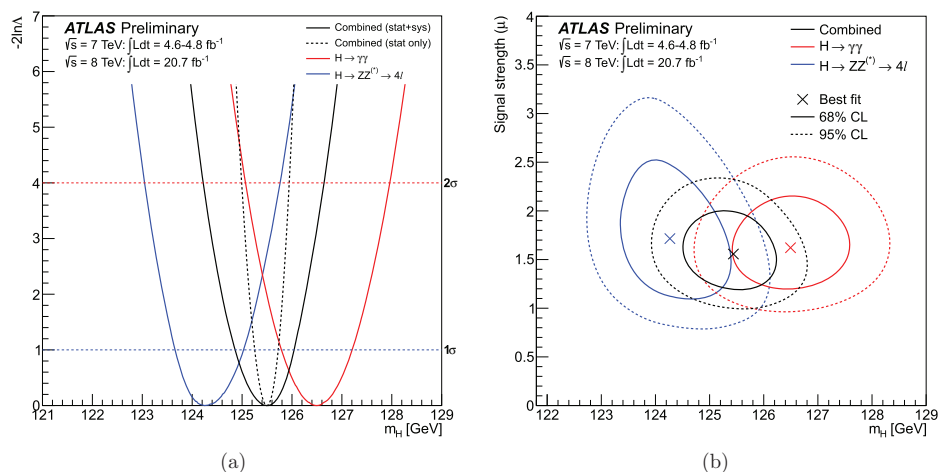


Fig. 2. – (a) The profile likelihood ratio as a function of m_H for the $H \rightarrow ZZ^{(*)} \rightarrow \ell^+\ell^-\ell^+\ell^-$ and $H \rightarrow \gamma\gamma$ channels and for their combination. (b) Confidence level intervals in the (μ, m_H) plane for the $H \rightarrow ZZ^{(*)} \rightarrow \ell^+\ell^-\ell^+\ell^-$ and $H \rightarrow \gamma\gamma$ channels and for their combination.

the various production modes to their SM values. Leading source of systematic uncertainties comes from the energy and momentum scale systematics. The profile likelihood ratio as a function of m_H and the confidence intervals in the (μ, m_H) plane are shown in fig. 2. The combined mass is measured to be

$$(1) \quad m_H = 125.5 \pm 0.2(\text{stat})_{-0.6}^{+0.5}(\text{sys}).$$

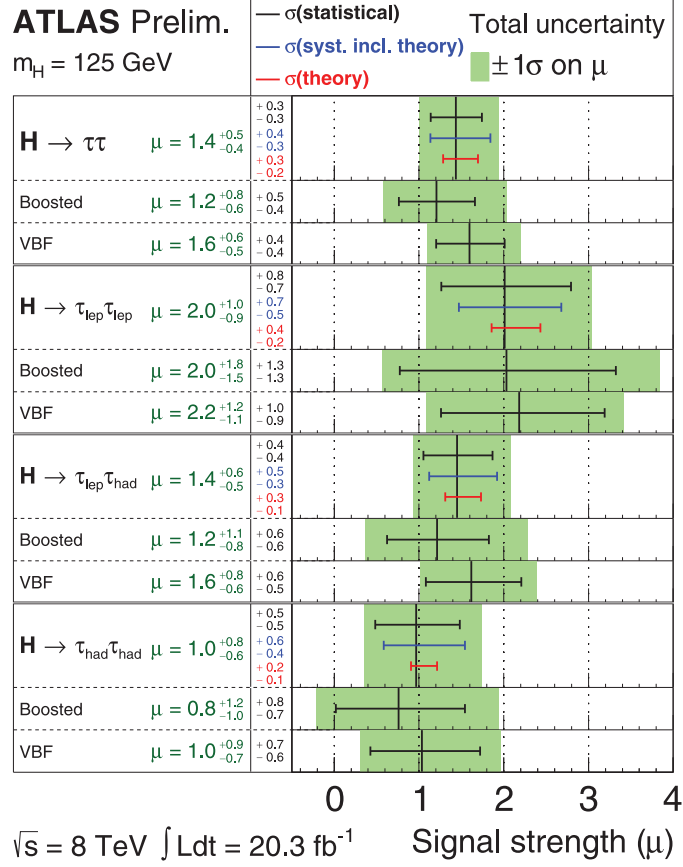


Fig. 3. – The best-fit value for the signal strength μ for the individual $H \rightarrow \tau\tau$ channels and their combination.

3. – The $H \rightarrow \tau\tau$ channel

The search for the decays of the Higgs boson into a pair of τ leptons is performed on the data sample of 20.3 fb^{-1} collected at a center-of-mass energy of $\sqrt{s} = 7 \text{ TeV}$ [7]. Final states in all τ decay combination, hadronic and leptonic, are considered in the analysis. The events are further classified in two categories optimized for the different SM production mechanisms. In the VBF category the events are characterized by the presence of two jets with a large pseudorapidity separation. The *Boosted* category includes events failing the VBF category definition, and targets events with a boosted Higgs boson from the gluon fusion production mechanism. In this category the Higgs candidates must have a large transverse momentum ($p_T > 100 \text{ GeV}$). The signal/background separation is obtained with multi-variate analyses.

The observed (expected) deviation from the background-only hypothesis corresponds to a significance of 4.2 (3.1) standard deviations. The measured signal strength is $\mu = 1.4^{+0.5}_{-0.4}$. This result represents the evidence of the decays of the Higgs boson to a pair of τ leptons, with a rate consistent with the SM expectation for a Higgs boson with a mass of 125 GeV. The measured signal strength in each category, and combined, are shown in fig. 3.

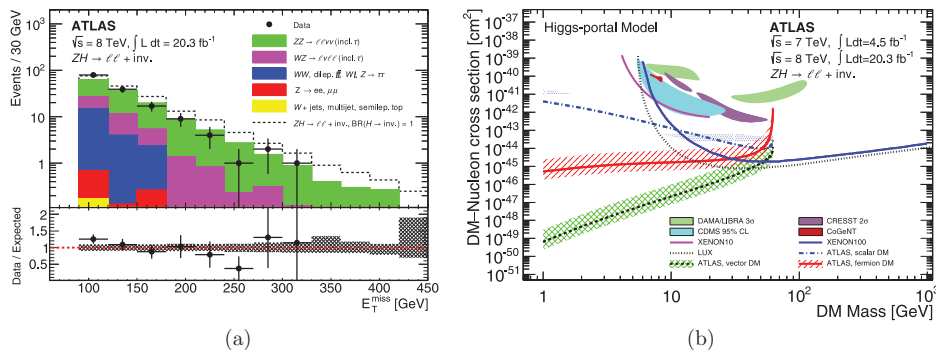


Fig. 4. – In (a) the distribution of E_T^{miss} after the full selection in the 8 TeV data is shown. The signal expectation for a Higgs boson with $m_H = 125.5$ GeV, a SM ZH production rate and $\text{BR}(H \rightarrow \text{inv.}) = 1$. The ratio of the data to the combined background expectation is shown in the inset at the bottom. In (b) the limits on the DM-nucleon scattering cross section are shown at 90% CL extracted from the $\text{BR}(H \rightarrow \text{inv.})$ in a Higgs portal scenario, compared to results from direct-search experiments. Cross section limits and favored regions correspond to a 90% CL unless stated otherwise [9].

4. – Search for invisible decays in associated production

Some extensions of the SM foresee Higgs boson decays to a pair of stable long-lived particles, with very small interaction cross sections with SM particles and not observable in the ATLAS detector, such as dark matter (DM) candidates. The search for these decays is performed in the case of a Higgs boson produced in association with a Z boson. The mass of the Higgs boson is taken to be $m_H = 125.5$ GeV, the best-fit value from the ATLAS experiment [8]. In fig. 4(a) the distribution of the E_T^{miss} after the full event selection for the 8 TeV data is shown. Limits on the cross section times BR for a Higgs boson decaying to invisible particles are set using a maximum likelihood fit to the E_T^{miss} distribution. Limits can be set for any Higgs boson mass, and the range $110 < m_H < 400$ GeV is considered in [10]. No deviation from the SM expectation is observed. For the discovered Higgs boson with $m_H = 125.5$ GeV, an upper limit of 75% at 95% CL is set on the BR to invisible particles. The expected SM limit in the absence of decays to invisible particles is 62% at 95% CL.

In fig. 4(b) the cross section results, interpreted within the context of a Higgs-portal DM scenario is shown [11]. In this scenario, in which the Higgs boson acts as the mediator particle between DM and SM particles, the Higgs boson can decay to a pair of DM particles. In this case the limit on the $\text{BR}(H \rightarrow \text{inv.})$ can be interpreted as an upper limit on the DM-nucleon scattering cross section [12-14]. Figure 4(b) shows 90% CL upper limits on the DM-nucleon scattering cross section for three different models in which the DM candidate is either a scalar, a vector, or a Majorana fermion.

5. – Couplings fit

The measurement of the Higgs couplings to each of the SM bosons and fermions are of critical importance in understanding the properties of the new particle, and it is realised

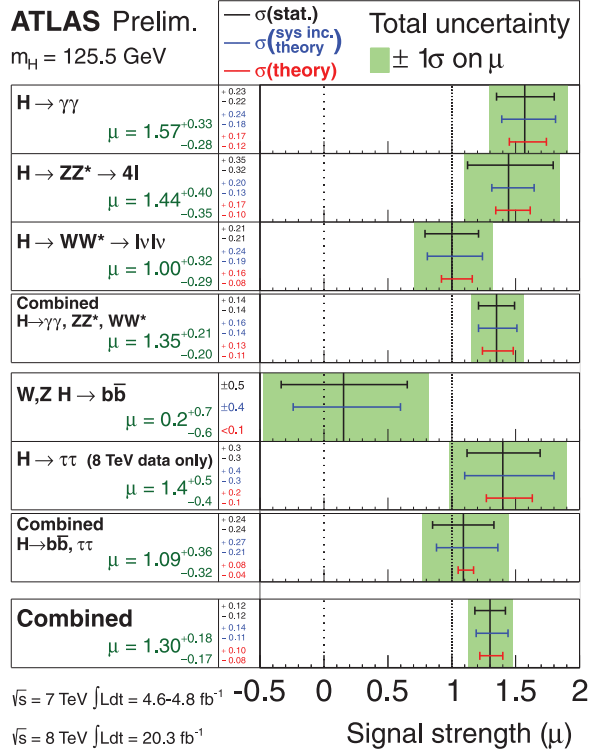


Fig. 5. – The measured signal strengths for a Higgs boson of mass 125.5 GeV, normalized to the SM expectations. The best fit values are shown by the solid vertical lines and the total $\pm 1\sigma$ uncertainties are indicated by the green shaded bands.

by combining the results of all decay channels analysed in ATLAS. The signal strengths for each channel, and combined, are shown in fig. 5.

The results presented here are based on the statistical model presented in [4, 15] and [16]. Measurements of couplings scale factors are implemented following the leading order framework described and motivated in [17]. The basic assumptions of the framework are that: the signals observed in each of the search channels originate from the same resonance with a mass close to 125.5 GeV; the width of the resonance can be neglected, thus allowing the $\sigma \times BR$ to be decomposed in:

$$(2) \quad \sigma \times BR(i \rightarrow H \rightarrow f) = \frac{\sigma_i \cdot \Gamma_f}{\Gamma_H};$$

and, only modifications of the couplings strengths are considered, assuming the tensor structure of the couplings to be the SM one. Different assumptions can be done on the couplings scale factors, corresponding to different benchmark models to be tested, for which results are reported in [16]. For the case in which the fit parameters are the scale factors κ_F for all fermions and κ_V for all vector couplings, the results of the fit are shown in fig. 6. No deviation from the expected SM values $\kappa_F = \kappa_V = 1.0$ is

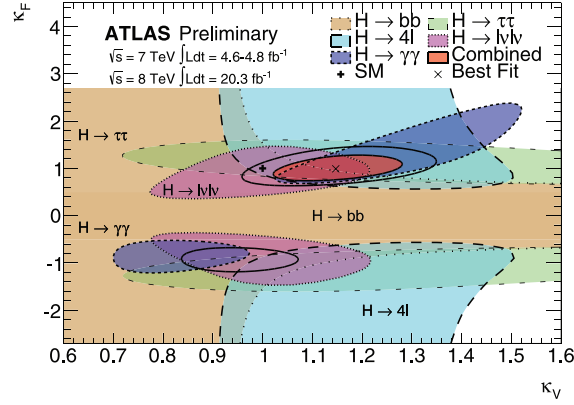
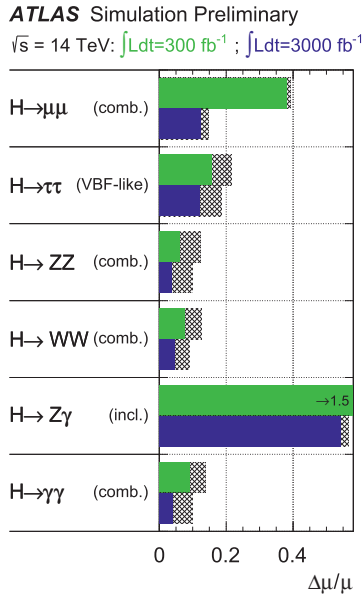
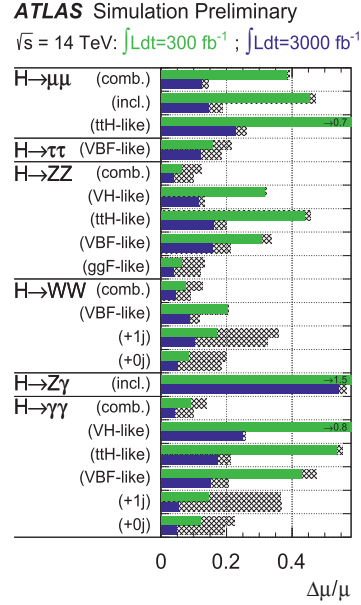


Fig. 6. – Results of the fit of the two parameters κ_V , κ_F in the 2-parameter benchmark model. The correlation of the two couplings scale factors is shown. The 68% CL contours are shown for the individual channels contributing to the measurement, and for their combination.

observed. Sensitivity to the relative sign of the two scale factors is gained only from the negative interference between the loop contributions of the W boson and the t quark in the $H \rightarrow \gamma\gamma$ decay.



(a)



(b)

Fig. 7. – Relative uncertainty on the signal strength for all Higgs final states, assuming a SM Higgs boson with a mass of 125 GeV and LHC at 14 TeV center-of-mass energy, and 300 fb^{-1} and 3000 fb^{-1} of integrated luminosity. In (a) the combined results are shown for each channel, indicating the combination of the different experimental subcategories outlined in (b).

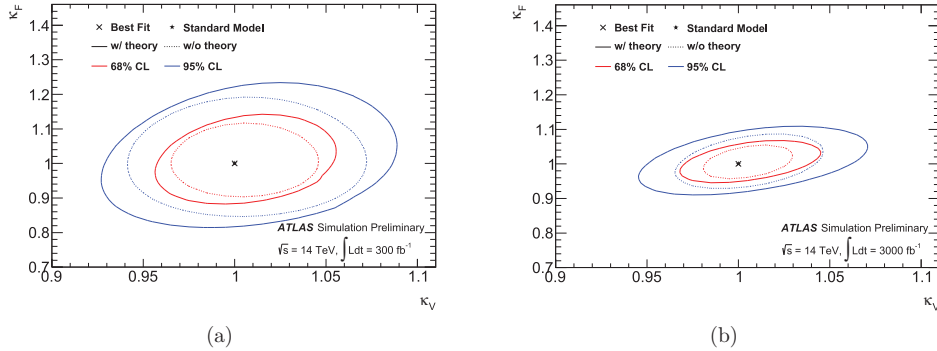


Fig. 8. – The 68% and 95% CL likelihood contours for κ_V and κ_F in a minimal coupling fit at a center-of-mass energy of 14 TeV and for an integrated luminosity of 300 fb^{-1} (a) and 3000 fb^{-1} (b).

6. – Projections at the next LHC runs

The present LHC programme is expected to deliver an integrated luminosity of about 300 fb^{-1} by the year 2022, with a peak instantaneous luminosity in the range of 2 to $3 \times 10^{34} \text{ cm}^{-2}\text{s}^{-1}$. The High-Luminosity LHC will deliver a total integrated luminosity of about 3000 fb^{-1} with a peak luminosity of $5 \times 10^{34} \text{ cm}^{-2}\text{s}^{-1}$.

Precision measurements in the Higgs sector are a priority also for the future Physics program of LHC. The ATLAS collaboration has presented a set of studies [18] in the briefing book of the European Strategy for Particle Physics [19]. Studies include projections for measurements at a center-of-mass energy of 14 TeV, with 300 fb^{-1} and, at the High-Luminosity LHC, with 3000 fb^{-1} .

All analyses have been projected to the foreseen run conditions, taking into account also the higher pileup levels, with average number of pileup events per bunch crossing of 50–60 in the first period, and 140 in the second high-luminosity period.

The results, in terms of expected uncertainties on the signal strength per channel, and combined, are shown in fig. 7. The expected results of the fit to the κ_F and κ_V scale factors of the couplings to all fermions and all vector bosons, are shown in fig. 8.

7. – Conclusions

Some of the main results of Run-1 measurements of the Higgs boson properties, with the ATLAS experiment at LHC, have been presented. The results show the status of the analyses as of April 2014. No deviation from the SM expectations has been found. Prospects in the field of Higgs properties measurements, with the data that will be collected at the future LHC runs, including the High-Luminosity LHC, have also been presented.

REFERENCES

- [1] ENGLERT F. and BROUT R., *Phys. Rev. Lett.*, **13** (1964) 321.
- [2] HIGGS P. W., *Phys. Rev. Lett.*, **13** (1964) 508.
- [3] GURALNIK G., HAGEN C. and KIBBLE T., *Phys. Rev. Lett.*, **13** (1964) 585.

- [4] ATLAS COLLABORATION, *Phys. Lett. B*, **716** (2012) 1, arXiv:1207:7214 [hep-ex].
- [5] CMS COLLABORATION, *Phys. Lett. B*, **716** (2012) 30, arXiv:1207:7235 [hep-ex].
- [6] ATLAS COLLABORATION, *JINST*, **3** (2008) S08003.
- [7] ATLAS COLLABORATION, ATLAS-CONF-2013-108 28 November 2013.
- [8] ATLAS COLLABORATION, ATLAS-CONF-2013-014 06 March 2013.
- [9] FOX P. J., KOPP J., LISANTI M. and WEINER N., *Phys. Rev. D*, **85** (2012) 036008.
- [10] AAD G. *et al.* (ATLAS COLLABORATION), *Phys. Rev. Lett.*, **112** (2014) 201802, 20 May, arXiv:1402.3244v3 [hep-ex].
- [11] PATT B. and WILCZEK F., arXiv:hep-ph/0605188.
- [12] FOX P. J., HARNIK R., KOPP J. and TSAI Y., *Phys. Rev. D*, **85** (2012) 056011.
- [13] KANEMURA S., MATSUMOTO S., NABESHIMA T. and OKADA N., *Phys. Rev. D*, **82** (2010) 055026.
- [14] DJOUADI A., LEBEDEV O., MAMBRINI Y. and QUEVILLON J., *Phys. Lett. B*, **709** (2012) 65.
- [15] ATLAS COLLABORATION, *Phys. Lett. B*, **726** (2013) 88, arXiv:1307.1427 [hep-ex].
- [16] ATLAS COLLABORATION, ATLAS-CONF-2014-009 May 2014.
- [17] LHC HIGGS CROSS SECTION WORKING GROUP, HEINEMEYER S., MARIOTTI C., PASSARINO G. and TANAKA R. (Editors), *Handbook of LHC Higgs Cross Sections: 3. Higgs Properties*, arXiv:1307.1347 [hep-ph].
- [18] ATLAS COLLABORATION, ATLAS-PHYS-PUB-2012-004.
- [19] ALEKSAN R. *et al.*, CERN-ESG-005.